The Astrophysical Journal, 629:1183–1187, 2005 August 20

THE ULTRAVIOLET TO NEAR-INFRARED OPTICAL PROPERTIES OF POLYCYCLIC AROMATIC HYDROCARBONS: A SEMIEMPIRICAL MODEL

A. L. Mattioda,[1,2] L. J. Allamandola,[1] and D. M. Hudgins[1]

Received 2005 March 8; accepted 2005 April 19

ABSTRACT

Interstellar polycyclic aromatic hydrocarbon (PAH) infrared emission features represent an important and unique diagnostic tool of the chemical and physical conditions throughout the universe. However, one challenge facing the widely accepted PAH emission model has been the detection of infrared features in regions of low UV flux. Using recently published laboratory near-infrared (NIR) PAH ion absorption data measured in our laboratory, we build on previous models for PAH ion absorption in the UV–visible to extrapolate a new model that incorporates PAH ion absorption in the NIR. This model provides a basis for comparing the relative energy absorption of PAH ions in the UV-visible and NIR regions for a wide variety of stellar types. This model demonstrates that the radiation from late-type stars can pump the mid-IR PAH features.

Subject headings: astrochemistry — infrared: ISM — ISM: molecules — methods: laboratory — molecular processes — techniques: spectroscopic

1. INTRODUCTION

The full extent to which the polycyclic aromatic hydrocarbon (PAH) emission features can be used as probes of many objects, galactic and extragalactic, has been revealed by the unprecedented sensitivity and mid-IR spectroscopic capabilities of the *Spitzer Space Telescope*. In less than a year, it has discovered new members of the PAH emission band family, enabled measurements of PAH band variations across faint, extended objects, and detected evidence for the PAH bands in galaxies with redshifts as high as $z = 2$ (Armus et al. 2004; Spoon et al. 2004; Smith et al. 2004a; Werner et al. 2004; Morris et al. 2004). These apparently omnipresent infrared emission features represent unique and important diagnostics of the chemical and physical conditions throughout the universe.

After two decades of observations, theoretical modeling, and laboratory measurements, it is now widely recognized that emission from mixtures of highly vibrationally excited PAHs and PAH ions can accommodate the general pattern of band positions, intensities, and profiles observed in the interstellar IR emission spectra. These provide insight into the detailed nature of the emitting PAH population and reflect conditions within the emitting regions, giving this population great potential as probes of astrophysical environments. For reviews of the observational and laboratory work, see Peeters et al. (2004), Hudgins & Allamandola (2004), and van Dishoek (2004); for theoretical models see Li (2004), Verstraete et al. (2001), Bakes et al. (2001), Draine & Li (2001), Li & Draine (2001), and Pech et al. (2002).

While a significant effort has been made to understand the global *infrared* spectral properties of PAHs under conditions appropriate to the emission zones, significantly less attention has been directed to understanding the IR fluorescence process by which cold, isolated PAH molecules in their neutral and ionized forms convert absorbed UV/visible/near-IR energy to emitted mid-/far-IR energy. Instead, most experimental studies of the electronic spectroscopy of PAHs and PAH ions in the UV, visible, and near-IR (NIR) regions have focused on testing the hypothesis that PAHs are responsible for some of the discrete diffuse interstellar bands (DIBs) that span the visible and near-IR spectral regions (e.g., Salama et al. 1996; Bréchignac & Pino 1999; Biennier et al. 2003).

Since the IR emission bands were initially found to be associated with UV-rich objects and PAHs absorb most strongly in the UV, it was tacitly assumed that they were pumped primarily by UV photons. To better understand this, Uchida et al. (1998, 2000) carried out a careful observational study of PAH emission from reflection nebulae pumped by different stellar types, some with a low ratio of ultraviolet to total flux. These observations showed that PAH emission is largely independent of stellar type for B- to F-type stars, and, for vdB 133, Uchida et al. (1998) showed that the interstellar infrared emission bands did not require an excitation spectrum dominated by ultraviolet excitation. Furthermore, the PAH emission bands were detected in a region of M31 for which the UV flux relative to the visible/NIR flux is even lower than for vdB 133 (Pagani et al. 1999). Smith et al. (2004b) observed the 3.3 μm PAH band in UV-poor debris disks, and back in 1983, Aitken & Roche (1983) recognized that UV was insufficient to pump the PAH features. Given the assumption that the emission process required substantial UV radiation and the paucity of experimental data on the overall electronic spectral properties of PAHs taken under appropriate astronomical conditions, the low fraction of UV available appeared to pose a problem for the PAH model.

To address this question, we measured the near-IR (NIR) spectra of PAH ions ranging in size from $C_{14}H_{10}$ to $C_{50}H_{22}$ (Mattioda et al. 2005, hereafter MHA05). In addition to their strong UV and visible transitions, all the ionized PAHs we have studied to date have strong, broad electronic absorption bands in the NIR. This paper summarizes the findings of MHA05 and develops a mathematical model of the IR emission pumping mechanism that incorporates these new data.

2. SUMMARY OF PAH NEAR-INFRARED SPECTROSCOPIC PROPERTIES

The NIR spectra of 27 different argon matrix–isolated PAH ions, ranging in size from 14 to 50 C atoms, are reported in MHA05. Most of the spectra tend to be dominated by a single

[1] NASA Ames Research Center, Mail Stop 245-6, Moffett Field, CA 94035-1000; amattioda@mail.arc.nasa.gov.
[2] SETI Institute, 515 North Whisman Road, Mountain View, CA 94043.

strong band or a cluster of strong bands falling between 13000 and 8000 cm^{-1} (0.77–1.25 μm). Anion bands, when present, tend to be substantially weaker than those of the corresponding cation. Given the astrophysical importance of quantitative band strengths, these were also determined. All the spectra reported by MHA05 show that PAH ions have NIR transitions that warrant consideration when describing the excitation process.

Comparisons between gas-phase and matrix isolation spectroscopic studies in the UV through NIR have shown that matrix effects slightly shift PAH *electronic* transitions (e.g., MHA05 and references therein). Consequently, UV–NIR astronomical spectra should not be directly compared with matrix spectra if the analysis requires precision at the part per thousand level or greater (e.g., assignment of specific DIB carriers). However, since the typical matrix shifts are small (<2%) and the overall PAH spectroscopic properties are retained, matrix data are very well suited to the task at hand—understanding the global PAH electronic transitions that span the UV through NIR region and drive the interstellar IR fluorescence process. The situation for the mid-IR emission features is strikingly different. Mid-IR comparisons with gas-phase measurements and quantum chemical calculations have shown that matrix perturbations of PAH *vibrational* transitions are insignificant in the context of the astronomical problem. Since it is those transitions that give rise to the well-known interstellar PAH emission, direct comparisons of matrix isolation data to astronomical spectra are appropriate (e.g., Hudgins & Allamandola 2004; Mattioda et al. 2003).

3. MATHEMATICAL MODEL OF PAH OPTICAL PROPERTIES

Thorough summaries of the literature applicable to the electronic properties of ionized PAHs can be found in MHA05 and Malloci et al. (2004). Malloci et al. (2004) present an outstanding study of computed PAH electronic absorption properties for select PAHs spanning the size range C_{10} to C_{48} from nearly zero to 30 eV. The overall electronic absorption properties of neutral, small PAHs, i.e., steeply dropping from the UV through the visible (e.g., Birks 1970), have been very well approximated in the PAH emission model developed by Draine & Li (2001) and Li & Draine (2001). The wavelength-dependent absorption cross section for a 50 C atom PAH, determined using the Li & Draine (2001, 2002) model, is plotted in Figure 1. However, as shown by MHA05 and illustrated in Figure 1, molecular-sized, open-shell species such as PAH ions have significant absorption features at considerably longer wavelengths than predicted by the model. Here we develop several mathematical expressions that take these new empirical data into account and that can then be used to model PAH electronic absorption properties.

In their thorough treatment of the IR emission process from interstellar PAHs, Li & Draine (2001, 2002) demonstrated that PAH absorption cross sections can be modeled by the following series of equations, expressed as the absorption cross section per C atom or $\sigma_{\rm abs}^{\rm PAH}/N_{\rm C}$ ($C_{\rm abs}^{\rm PAH}/N_{\rm C}$ in Li & Draine):

$$\frac{\sigma_{\rm abs}^{\rm PAH}(\lambda)}{N_{\rm C}} = 34.58\times10^{-18-3.431X}\,\frac{\rm cm^2}{\rm C\ atom} + \sum_{j=1}^{2} S_j(\lambda), \quad (1)$$

where $X = \lambda/\mu$m, with the wavelength λ expressed in μm, over the wavelength range 0.1 μm $< \lambda <$ 3.3 μm and S_j represents Drude profiles described by

$$S_j(\lambda) = \frac{2}{\pi}\,\frac{\gamma_j\lambda_j A_{{\rm int},j}}{(\lambda/\lambda_j - \lambda_j/\lambda)^2 + \gamma_j^2}. \quad (2)$$

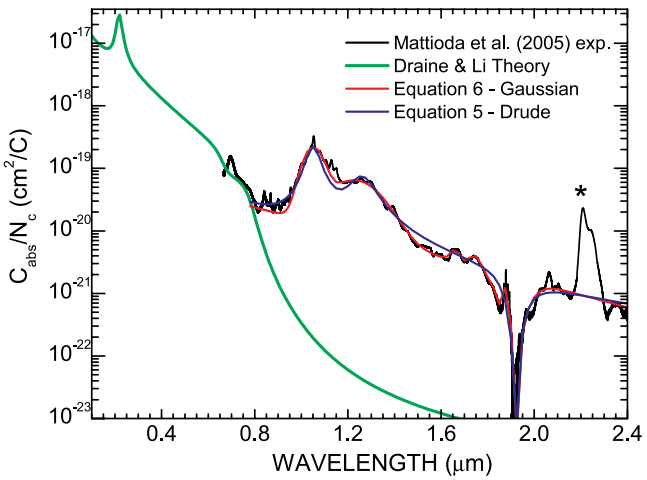

FIG. 1.—Comparison of the Li & Draine (2002) model (*green line*) with the experimental average NIR cross section (*black line*) for the PAH ions measured by MHA05. This comparison shows that ionized PAHs absorb with substantial strength at significantly longer wavelengths than predicted for the modeled generic "astronomical PAHs." Also shown are the NIR model spectra described by eqs. (5) (*blue line*) and (6) (*red line*) in the text. The asterisk denotes an artifact introduced by the spectrometer's beam splitter.

For this equation, γ_j is a broadening parameter, λ_j is the central wavelength of a feature in μm, and $A_{{\rm int},j}$ is the integrated absorption strength expressed in cm C^{-1} ($\sigma_{{\rm int},j}$ in Li & Draine). Equation (1) produces a continuous cross section baseline that drops with increasing wavelength, mimicking the falloff in PAH ion absorption cross section with wavelength, and equation (2) describes features superposed on that continuum. These are adapted from equations (11) and (12), respectively, in Li & Draine (2001). To account for the variation of the absorption spectrum as a function of PAH size and charge, in their model, Li & Draine (2001) further adopted the cutoff function of Désert et al. (1990),

$$\mathrm{cutoff}(\lambda,\lambda_c) = \frac{1}{\pi}\arctan\left[\frac{10^3(y-1)^3}{y}\right] + \frac{1}{2}, \quad (3)$$

in which $y = \lambda_c/\lambda$ and the cutoff wavelength λ_c was derived from Salama et al. (1996) and is defined as

$$\lambda_c(\mu{\rm m}) = 1/(2.282M^{-0.5} + 0.889) \quad (4)$$

for PAH cations, where M (the number of fused benzenoid rings) is $\sim 0.4N_{\rm C}$ for $N_{\rm C} > 40$ and $\sim 0.3N_{\rm C}$ for $N_{\rm C} < 40$ ($N_{\rm C}$ is the number of carbon atoms).

These equations are a good representation of the then-known PAH absorption properties from the far UV through most of the visible wavelength range. As can be seen in Figure 1, while this extended into the NIR, the PAH absorption cross sections dropped precipitously. Nonetheless, with these equations, Li & Draine (2002) showed that the observed PAH emission from vdB 133 could be reproduced. However, as Draine & Li (2001) pointed out, high-quality absorption spectra for many PAH ions were not available in the literature at the time, and extrapolation through the NIR had to be made. With the publication of the many NIR PAH ion spectra by MHA05, this issue warrants revisiting.

Along with the wavelength-dependent absorption cross sections for the 27 PAHs reported by MHA05, Figure 1 shows that PAH ions possess significant absorption in the NIR at wavelengths well beyond the cutoff wavelength predicted by Désert

TABLE 1
PARAMETERS FOR DRUDE AND GAUSSIAN PROFILES IN EQUATIONS (5) AND (6)

Gaussian (G)/Drude (S) Parameter	$\lambda_0(\mu m)/\lambda_j(\mu m)$	$w(\mu m)/\gamma_j$	$A(cm^2\ \mu m\ C^{-1})/A_{int,j}(cm^2\ \mu m^{-1}\ C^{-1})$
G_1	1.05	0.0805	2.0×10^{-20}
G_2	1.23	0.20	1.4×10^{-20}
G_3	1.66	0.0370	8.0×10^{-23}
G_4	1.745	0.0450	8.4×10^{-23}
G_5	1.885	0.0150	4.6×10^{-23}
G_6	1.90	0.135	3.22×10^{-22}
S_1	1.05	0.12	1.20×10^{-20}
S_2	1.26	0.18	4.5×10^{-21}
S_3	1.915	0.13	6.85×10^{-23}

NOTE.—Parameters were determined based on the data in MHA05.

et al. (1990). Even relatively small PAHs have significant absorption near 1 μm, well to the red of the model-determined cutoff. This also holds for the predicted cutoff of much larger PAHs. For example, the predicted cutoff wavelength for a 200-C-atom–containing PAH is only about 0.8 μm (Li & Draine 2002). As shown in Figure 1, for most of the PAH ions studied, the absorptions cover a broad region of the NIR and tend to peak between 0.8 and 1.5 μm.

Following Li & Draine (2001, 2002), we consider the merits of the two following equations to model the NIR cross sections of ionized PAHs from 0.8 to 2.4 μm:

$$\frac{\sigma_{abs}^{PAH}(\lambda)}{N_C} = 3.5 \times 10^{-19-1.45\lambda/\mu m} \frac{cm^2}{C\ atom} + S_1 + S_2 - S_3, \quad (5)$$

$$\frac{\sigma_{abs}^{PAH}(\lambda)}{N_C} = 1.5 \times 10^{-19-\lambda/\mu m} \frac{cm^2}{C\ atom} + G_1 + G_2 + G_3 + G_4 + G_5 - G_6, \quad (6)$$

where λ is the wavelength in μm. The first term in equations (5) and (6) establishes a continuous baseline that drops with increasing wavelength, while the additional terms describe the broad bands peaking near 1.05 and 1.23 μm evident in the experimental data. Based on the available experimental data, there does not appear to be a significant cutoff wavelength (see Fig. 1). Instead, the underlying continuum gradually decays until approximately 2.4 μm, the edge of the experimental data available (MHA05). One will note a striking dip in the baseline centered near 1.9 μm. This break is narrow, spanning the range from 1.79 to 2.09 μm, and, since the experimental curve presented in Figure 1 is a composite of multiple spectra, represents a real dip in the NIR features of the PAH ions studied. Thus, here we assume that this break in the underlying continuum is a general characteristic of the NIR properties of PAH ions, and it is modeled in the equations above through the subtraction of the appropriate function (G_6). Equation (5) uses the well-known Drude profiles (see eq. [2]) to describe the broad bands in the region, while equation (6) uses Gaussian profiles for these features (see eq. [7]). Both equations are represented in Figure 1.

The additional Gaussian terms in equation (6) (G_3, G_4, and G_5) allow for completeness of fit to the weaker features in the experimental data and may be excluded at the reader's (modeler's) discretion. Parameters for the Drude and Gaussian profiles are located in Table 1.

The Gaussian functions for equation (6) are described by

$$G = \frac{A}{w\sqrt{\pi/2}} e^{-2(\lambda-\lambda_0)^2/w^2}, \quad (7)$$

where λ_0 is the center of the peak in μm, w is 2 times the standard deviation of the Gaussian distribution (2 σ) or approximately 0.849 times the width of the peak at half height in μm, and A is the area under the peak.

As shown in Figure 1, the Gaussian profiles provide a much better fit of the experimental data than do the corresponding Drude profiles, as evident in the fitting of the bands around 1.05 and 1.25 μm. This difference is likely fundamental in nature, since the experimental data pertain to transitions in mostly planar, two-dimensional species (Rouleau et al. 1997). Strictly speaking, Drude profiles are associated with three-dimensional species. Thus, while it is common in astrophysics to use Drude profiles to describe the optical properties of dust particles, for the NIR properties of collections of PAH ions it appears that a Gaussian function is more appropriate.

In summary, a complete model for the PAH ion absorption cross section from the far-UV through the NIR can be obtained by combining Draine and Li's formulation (eq. [1] above), which is valid for the region from about 0.05 to 0.78 μm, with our equation (6) (or eq. [5]), which is valid from 0.78 to 2.4 μm.

4. IMPACT OF PAH ION NIR PROPERTIES ON PUMPING THE IR EMISSION FEATURES

Here we evaluate the possibility that the PAH emission features could be vibrationally excited by stellar NIR photons.

The fraction of available stellar energy absorbed by an optically thick cloud of PAHs was determined by convoluting the stellar output (blackbody), from a star of given type, with the model absorption function described in § 3. Figure 2 presents the UV through NIR stellar output for a variety of different star types, the model PAH ion absorption function from above, and the convolution of the two. The integrated amount of radiant energy absorbed by these PAH ions is indicated by the colored areas in Figure 2 (*green*, UV; *blue*, visible; *red*, NIR). While the convolved function represents the amount of energy absorbed per carbon atom per wavelength, the area gives the total amount of radiant energy absorbed per C atom. As noted in § 3, the Draine and Li equation (eq. [1]) covers the UV and visible portions of the electromagnetic spectrum (up to 0.78 μm), while equation (6) covers the NIR portion out to 1.9 μm. The 1.90 μm cutoff was chosen since it represents the position of the apparent break in the underlying continuum and represents a convenient dividing line between the near- and mid-IR spectroscopic regions.

From the convolved data curves in Figure 2, one can clearly see that as stellar temperature decreases, the amount of energy absorbed by PAH ions in the NIR relative to the amount absorbed in the UV and visible increases markedly. To quantitatively

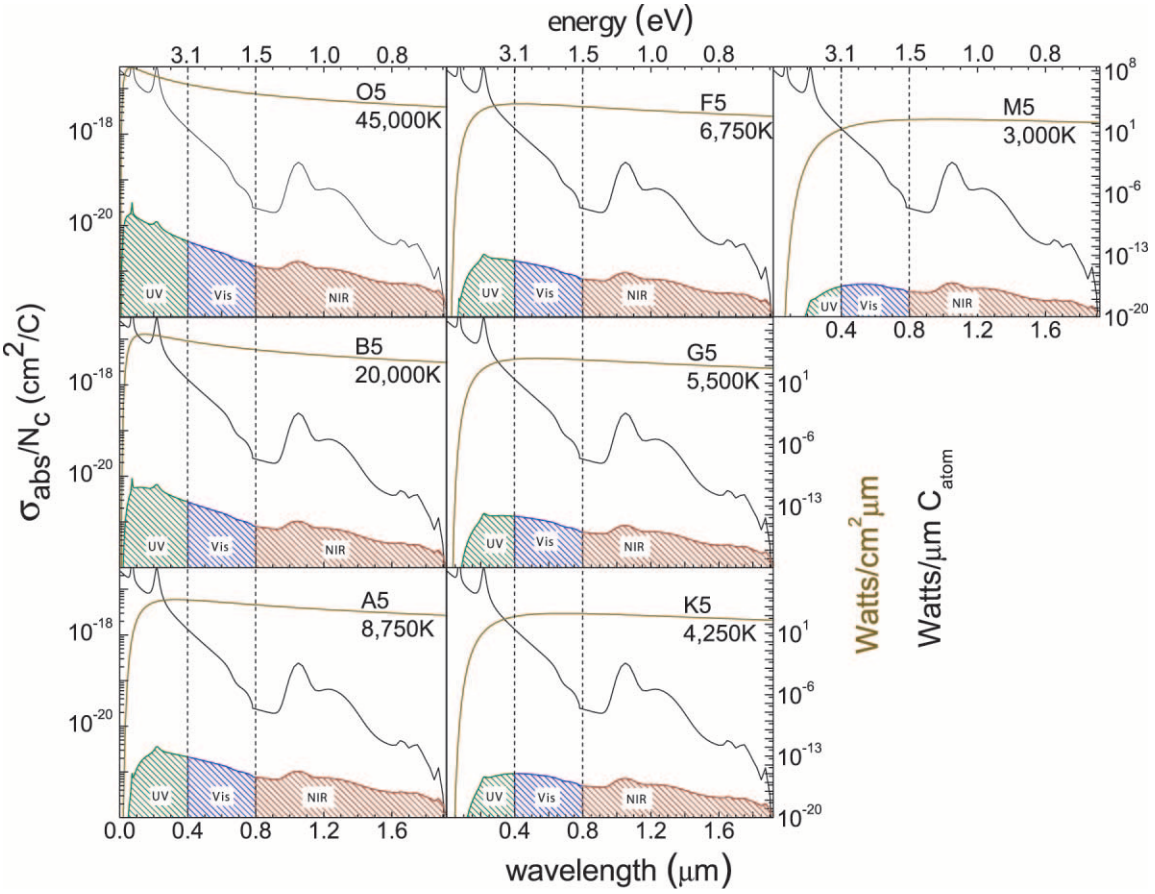

FIG. 2.—Stellar radiative energy absorbed by PAHs as a function of star type. The UV through NIR stellar (blackbody) output for a variety of different star types (*tan line*, right tan axis units) is plotted in conjunction with the PAH ion absorption cross section described in § 3 (*black line*, left axis units). The integrated amount of radiant power absorbed by an optically thick cloud of PAH ions is indicated by the filled area (right black axis units: *green*, UV; *blue*, visible; *red*, NIR). PAH ion UV–visible absorption is modeled using the Li & Draine (2002) formalism for a 50 carbon atom PAH, and NIR absorption is modeled using eq. (6). The vertical lines at 0.4 and 0.78 μm demarcate the UV–visible and visible–NIR spectral regions.

evaluate the relative importance of these wavelength regimes in pumping the mid-IR emission features, we compare the convolved areas from 0 to 0.4 μm for the UV fraction, from 0.4 to 0.78 μm for the visible, and from 0.78 to 1.90 μm for the NIR fraction in Figure 3. This shows that the power absorbed in the NIR becomes nearly equivalent to the power absorbed in the UV and visible around 4000 and 3000 K, respectively. Using Kurucz model radiation curves, instead of blackbody, for this analysis would only serve to enhance the importance of the NIR in pumping the PAH emission features, since Kurucz models typically decrease the flux at UV wavelengths for low-temperature stars.

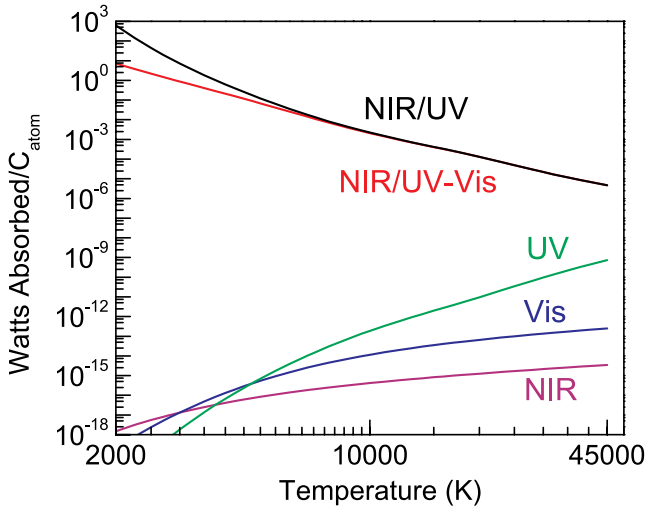

FIG. 3.—Power delivered to PAH ions by UV, visible, and NIR photons as well as the NIR/UV–visible and NIR/UV ratios plotted as a function of stellar temperature.

A quantity not readily visible in Figure 2 is the integrated amount of NIR energy absorbed by PAH ions. Figure 3 displays the UV, visible, and NIR power absorbed per carbon atom as a function of stellar temperature. The power absorption for these various regions can be modeled using one of the three equations

$$y = A + BT + CT^2 + DT^3, \quad (8)$$

$$y = A + BT, \quad (9)$$

$$y = AT^B, \quad (10)$$

where T is the stellar temperature (K) and A, B, C, and D are parameters provided in Table 2. The appropriate stellar temperature ranges, parameters, and spectroscopic regions for each equation are listed in Table 2. The equations reproduce the curves with a correlation coefficient of at least 0.9997, except for the low-temperature regime in the visible curve for which the correlation coefficient is 0.9983 (a correlation coefficient of 1 represents a perfect fit).

From Figure 3 one can see that the amount of NIR energy absorbed by an optically thick cloud of PAH ions approaches that

TABLE 2
Parameters for UV, Visible, and NIR Energy Absorption Equations

	UV		Visible		NIR	
Parameter	Eq. (10)	Eq. (8)	Eq. (10)	Eq. (8)	Eq. (8)	Eq. (9)
Temperature (K)	1300–11000	11000–45000	1300–11000	11000–45000	1300–11000	11000–45000
A	1.894×10^{-41}	-1.03×10^{-10}	2.3×10^{-29}	-1.67×10^{-14}	3.1×10^{-17}	-4.88×10^{-16}
B	7	2.00×10^{-14}	3.67	1.18×10^{-18}	-3.67×10^{-20}	8.77×10^{-20}
C	...	-1.28×10^{-18}	...	$1.79 \times 10-^{22}$	1.14×10^{-23}	...
D	...	2.77×10^{-23}	...	-1.68×10^{-27}	-3.9×10^{-28}	...

of the UV–visible at stellar temperatures below about 8000 K. However, it becomes greater than the UV energy input at stellar temperatures below 4000 K (see NIR/UV ratio in Fig. 3). In addition, in Figure 3 one can see that the ratio of NIR/UV–visible energy absorbed by PAH ions decreases almost linearly with increasing temperature. In fact, the NIR/UV–visible ratio can best be fitted with two linear functions,

$$\log\left(\frac{\mathrm{NIR_{absorbed}}}{\mathrm{UV\text{–}vis_{absorbed}}}\right) = -5.08 \log T + 17.64, \quad \text{for } 3000\ \mathrm{K} < T < 9000\ \mathrm{K}, \tag{11}$$

$$\log\left(\frac{\mathrm{NIR_{absorbed}}}{\mathrm{UV\text{–}vis_{absorbed}}}\right) = -4.14 \log T + 13.8, \quad \text{for } T > 9000\ \mathrm{K}. \tag{12}$$

Equation (11) is best used for temperatures between 3000 and 9000 K and has a correlation coefficient of 0.9997. Equation (12) addresses temperatures above 9000 K, with a correlation coefficient of 0.9999.

This behavior shows that while the availability of UV-visible photons to pump the PAH emission features drops with decreasing star type, the contribution by the stellar NIR photons remains steady and actually becomes comparable to that of the higher energy photons for the latest type stars. Inspection of the integrated power curves in Figure 2 shows that the net effect of decreasing stellar temperature is a steady but slow and gradual decrease in the integrated radiative power pumped into the PAH ions and a concomitantly slow decrease in the power emitted in the mid-IR by the PAH bands, not a precipitous drop. This predicts that, if present in the vicinity of even very late type stars, PAH ions can be vibrationally excited by the stellar radiation field, and their contribution to the mid-IR from these objects will decrease "not with a bang but a whimper."

5. CONCLUSION

The publication of laboratory near infrared spectra for a wide variety of PAH ions has permitted a revision in the PAH ion absorption model for this region. A new model, which takes into account the significant NIR absorption features of PAH ions, has been proposed. Based on this new model and in conjunction with the Draine and Li UV–visible model, a comparison is made between the energy absorbed by PAH ions in the NIR and that of the UV–visible region for a wide array of stellar classes, based on blackbody radiation fields. This comparison reveals that for lower temperature stars, NIR energy absorption becomes increasingly important, matching the energy absorbed from the UV–visible for late K and M stars. Thus, even in areas of low UV flux, absorption in the NIR could stimulate mid-IR emission from PAH ions.

We acknowledge the National Research Council (NRC) and NASA's Long Term Space Astrophysics (LTSA, grant 399-20-40) and Astrobiology (grant 344-53-92) Programs for supporting this work as well as helpful comments from an anonymous referee. As always, we are indebted to Bob Walker for his outstanding technical support of all phases of the experimental work. We are indebted to Jan Cami for detailed discussions on stellar radiation fields. The quote, "not with a bang but a whimper" is from T. S. Elliot's "The Hollow Men."

REFERENCES

Aitken, D. K., & Roche, P. F. 1983, MNRAS, 202, 1233
Armus, L., et al. 2004, ApJS, 154, 178
Bakes, E. L. O., Tielens, A. G. G. M., & Bauschlicher, C. W. 2001, ApJ, 556, 501
Biennier, L., Salama, F., Allamandola, L. J., & Scherer, J. J. 2003, J. Chem. Phys., 118, 7863
Birks, J. B. 1970, Photophysics of Aromatic Molecules (London: Wiley)
Bréchignac, P., & Pino, T. 1999, A&A, 343, L49
Désert, F.-X., Boulanger, F., & Puget, J. L. 1990, A&A, 237, 215
Draine, B. T., & Li, A. 2001, ApJ, 551, 807
Hudgins, D. M., & Allamandola, L. J. 2004, in ASP Conf. Ser. 309, Astrophysics of Dust, ed. A. N. Witt, G. C. Clayton, & B. T. Draine (San Francisco: ASP), 665
Li, A. 2004, in ASP Conf. Ser. 309, Astrophysics of Dust, ed. A. N. Witt, G. C. Clayton, & B. T. Draine (San Francisco: ASP), 417
Li, A., & Draine, B. T. 2001, ApJ, 554, 778
———. 2002, ApJ, 572, 232
Malloci, G., Mulas, G., & Joblin, C. 2004, A&A, 426, 105
Mattioda, A. L., Hudgins, D. M., & Allamandola, L. J. 2005, ApJ, 629, 1188 (MHA05)
Mattioda, A. L., Hudgins, D. M., Bauschlicher, C. W., Jr., Rosi, M., & Allamandola, L. J. 2003, J. Phys. Chem. A, 107, 1486
Morris, P. W., Noriega-Crespo, A., Marleau, F. R., Teplitz, H. I., Uchida, K. I., & Armu, L. 2004, ApJS, 154, 339
Pagani, L., Lequeux, J., Cesarsky, D., Donas, J., Milliard, B., Loinard, L., & Sauvage, M. 1999, A&A, 351, 447
Pech, C., Joblin, C., & Boissel, P. 2002, A&A, 388, 639
Peeters, E., Allamandola, L. J., Hudgins, D. M., Hony, S., & Tielens, A. G. G. M. 2004, in ASP Conf. Ser. 309, Astrophysics of Dust, ed. A. N. Witt, G. C. Clayton, & B. T. Draine (San Francisco: ASP), 141
Rouleau, F., Henning, Th., & Stognienko, R. 1997, A&A, 322, 633
Salama, F., Bakes, E., Allamandola, L. J., & Tielens, A. G. G. M. 1996, ApJ, 458, 621
Smith, J. D. T., et al. 2004a, ApJS, 154, 199
Smith, T., Clayton, G., & Valencic, L. 2004b, AJ, 128, 357
Spoon, H. W. W., et al. 2004, ApJS, 154, 184
Uchida, K. I., Sellgren, K., & Werner, M. W. 1998, ApJ, 493, L109
Uchida, K. I., Sellgren, K., Werner, M. W., & Houdashelt, M. L. 2000, ApJ, 530, 817
van Dishoek, E. F. 2004, ARA&A, 42, 119
Verstraete, L., et al. 2001, A&A, 372, 981
Werner, M. W., Uchida, K. I., Sellgren, K., Marengo, M., Gordon, K. D., Morris, P. W., Houck, J. R., & Stansberry, J. A. 2004, ApJS, 154, 309